DIRECT NUMERICAL SIMULATION OF TURBULENT FREE-SURFACE FLOW

Tomoaki Kunugi
Dept. of Nuclear Engineering, Kyoto University
Yoshida, Sakyo, Kyoto, 606-8501, Japan

Shin-ichi Satake
Dept. of Mechanical System Engineering, Toyama University
Toyama, Toyama, 930-0887, Japan

Yasuo Ose
Dept. of Energy System, Japan Atomic Energy Research Institute
Tokai, Ibaraki, 319-1195, Japan

ABSTRACT

A direct numerical simulation (DNS) on a turbulent free-surface flow has been carried out to grasp and understand a gas-liquid interaction mechanism that is very important for the environmental problems and the industrial devices. The multi-interface advection and reconstruction solver (MARS) developed by one of the authors is applied to a turbulent free-surface flow. The initial velocity ratio of the gas- to the liquid-flow is assumed to be 100. The free-surface is deformed by the high shear stresses between two flows. Many ripples and small waves are generated on the free-surface and some of them are growing up to the big waves. Finally, many small ripples on the long wave, some breaking-up waves, some liquid-droplets in the gas flow and some bubbles in the liquid-flow are observed. The statistics of the turbulent quantities for the turbulent free-surface flow are presented. According to this preliminary computation, it can be summarized that the turbulent energy at the free-surface is mainly produced by the fluctuating wavy-motion of the free-surface and the turbulent convection, i.e., the fluctuations of surface-curvature and the high velocity change in the free-surface region.

INTRODUCTION

The turbulent behavior of liquid and gas flows at a free surface is not very well understood rather than the motions at the solid boundary, but these behaviors in the practical application are equally important. In addition, the mechanism of scalar transport into a turbulent liquid across the gas-liquid interfaces or free-surfaces is great importance in the industrial devices, especially a chemical processes like gas-absorption equipment etc. Recently, the turbulent mass transport of the carbon-dioxide is very important in the global-warming problem because of understanding the "Missing sink" in a mass balance of the carbon production and consumption after the industrial revolution.

There are many studies on the liquid-side turbulence near the free-surfaces imposed with no or very low shear flow such as Rashidi and Barnerjee (1988) and Komori et al. (1989). Moreover, experimental investigations with wind shear have been less performed. Thus, in case of the low wind velocity, most of all previous studies have been considered the turbulence structure caused by the shear rate in the liquid-side flow rather than the coupling effect between the gas- and liquid-flows. However, in case of the high wind velocity, the turbulent characteristics near the free-surface could be influenced by a deformation of the free-surface due to the strong wind shear.

DNSs for the turbulent free-surface flows in coupled gas-liquid flow and experimental investigations have been less extensive because of the numerical and experimental difficulties for the tracking and measuring the free-surface deformation. Recently, Lombardi et al. (1996) performed

the DNS with the coupling between gas- and liquid-flow motions, however, they still assumed the interface was maintained flat, i.e., this assumption similar to that of Lam and Barnerjee (1992). This assumption is too special and unrealistic for the general air-water system with high shear wind. Thus, until today, all of the previous investigations on turbulent free-surface flows with the shear wind were limited in the range of very small interfacial fluctuation.

Therefore, in order to understand the gas-liquid interaction at the turbulent free-surface, it is necessary to establish a precise free-surface tracking algorithm for two-phase flows and to obtain a high quality initial turbulent field for both gas- and liquid-flows via a time-dependent three-dimensional DNS.

In the present study, the DNS for the turbulent free-surface flow with the high wind shear has been carried out by means of the coupled gas-liquid flow solution procedure, i.e., MARS developed by Kunugi (1997). The turbulent statistics for the free-surface characteristics, pressure distribution, velocity fluctuations, two-point correlation, energy spectrum and budget of turbulent kinetic energy are presented.

PROBLEM DESCRIPTION

The physical problem treated here is the motion of two Newtonian incompressible fluids allowed the deformation of the interface between them. In Fig.1, the problem schematic view is shown. The computational domain is 9 m in width (x-direction), 4 m in height (y-direction) and 12 m in length (z-direction). The periodic boundary conditions in the spanwise (x) and streamwise (z) directions are imposed and the free-slip boundaries are applied to both upper and lower boundaries in y-direction. The initial free-surface is located at the mid-plane of the total height, i.e., y=2 m.

SOLUTION PROCEDURE

Following three important features for modeling the advection and reconstruction of the interfaces and free surfaces should be considered; 1) surface and interface should be tracking or capturing precisely with sufficient accuracy of the mass and volume conservation, 2) the advected mass and momentum fluxes of moving fluid-segments should be precisely conserved when the surface and interface are passing through the computational cells, 3) appropriate reconstruction procedure of surfaces and interfaces should be considered from the continuity point of view. Therefore, one of the authors has been developed a direct numerical procedure, i.e., the MARS (Multi-interface Advection and Reconstruction Solver by Kunugi (1997) for solving general multiphase flow problems with many free surfaces and interfaces. It consists of the continuum surface force (CSF) model (Brackbill et al., 1992) for surface tension as a volumetric force in the momentum equation and a simple piece-wise linear calculation algorithm for tracking and reconstructing the interfaces between neighborhood computational cells such as PLIC (Kothe et al., 1996 or Kunugi, 1997). The MARS meets these important features described above and includes an interfacial shear stress for the coupling of two fluids (such as gas and liquid) at the interfaces.

Surface Tension Model

The general form of the surface tension can be expressed as (Laandau and Lifshitz, 1993):

$$(P_1 - P_2 + \sigma\kappa)\hat{n}_i = (\tau_{1ik} - \tau_{2ik})\hat{n}_k + \frac{\partial\sigma}{\partial x_i}. \qquad (1)$$

Here, P_m is pressure of *m-th* fluid (m=1,2), σ is surface tension coefficient, $\hat{n} = n/|n|$ (here, $n = \nabla F$; F is a volume of fluid function) is unit normal vector to the m=2 fluid (here, $|n|$ is the norm), $\tau_{m.ik}$ is shear stress tensor and k is curvature of the surface.

The surface curvature κ is obtained by the unit normal vector $\hat{n}$ calculated from the F-values of surrounding cells as the same manner as the CSF model as follows:

$$\kappa = -(\nabla \cdot \hat{n}) = \frac{1}{|n|}\left[\left(\frac{n}{|n|}\cdot\nabla\right)|n| - (\nabla \cdot n)\right] \qquad (2)$$

Therefore, a body force $F_V(x)$ as the surface tension based on the CSF model can be written as,

$$F_V(x) = [\sigma\kappa(x) + \tau_2(x)_{ii} - \tau_1(x)_{ii}]n(x)\langle\rho(x)\rangle/\overline{\rho}, \qquad (3)$$

here, $\langle\rho\rangle$ is mean density of fluids ($=\sum_m \rho_m$), $\overline{\rho}$ is mean density at the surface/interface, $\overline{\rho} = (\rho_1 + \rho_2)/2$. The $\overline{\rho}$ is assumed to be a constant and varied with the both fluid densities based on the equation of states.

Volume Tracking

A slope of the surface ($\partial F/\partial x$) is considered when a transport fluid-flux $\delta F(=U\delta t$; U is a velocity in the upstream direction) is calculated based on the MARS (Kunugi , 1997). The following transport equation regarding the volume of mth-fluid F_m based on the one-field model (U_m=U) is used.

$$\frac{\partial F_m}{\partial t} + (U\cdot\nabla)F_m = \frac{\partial F_m}{\partial t} + \nabla\cdot(F_m U) - (F_m\cdot\nabla)U = 0 \qquad (4)$$

Governing Equations for Multiphase Flows

The continuity equation for m fluids can be expressed as:

$$\frac{\partial \langle F \rangle}{\partial t} + \sum \left[\nabla \cdot (F_m U) \right] = 0, \tag{5}$$

here, $\langle F \rangle = \sum F_m = 1$ and the momentum equation with the CSF model:

$$\frac{\partial U}{\partial t} + \nabla (UU) = G - \frac{1}{\langle \rho \rangle} \nabla P - \nabla \cdot \tau + \frac{1}{\langle \rho \rangle} F_V, \tag{6}$$

These governing equations can be solved by means of the well-known projection method. Once the velocity field can be obtained, the fluid can be transported by using the volume tracking procedure with the PLIC (Kothe et al., 1996) or the MARS (Kunugi, 1997).

COMPUTATIONAL CONDITIONS

The initial turbulent fields for both gas- and liquid-flows are obtained from the result of the time dependent 3D-DNS for a turbulent open-channel flow with non-slip bottom wall and free-slip at the free-surface (Satake, 1998). This turbulent field is applied to the gas flow and the inverse profile is imposed to the liquid phase. The mean velocity ratio of the gas- to liquid-flow is set to be 100, i.e., the specified mean velocities are 18.7 m/s for gas and 0.187 m/s for liquid, respectively. Since the free-surface is always deformed by the shear stresses in case of the high wind velocity, it is difficult to define an interfacial friction velocity. The number of grids is 144x64x192 in x-, y- and z-directions, respectively. The constant grid spacing is used; $\Delta x=\Delta y=\Delta z=0.0625$ m. Therefore, the spatial resolution of the free-surface wave is 0.125 m and is one of the limitations of this computation. The time increment of the integration for the governing equations is $\delta t=5\text{x}10^{-4}$ sec.

In general, it should be necessary to discuss the usage of the periodic boundary condition for this kind of turbulent boundary layer typed flows. Despite this difficulty caused by the limitation of computer memory, the authors applied the periodic boundary conditions to the developing free-surface flow in order to know the effects of surface wave deformation on the turbulent characteristics of it. In this sense, this computation should be stopped at certain time period that the thickness of boundary layer reaches the upper boundary of this computational domain. After many trial computations, the computational time period was taken to be 20 sec, i.e., 40,000 time steps.

RESULTS AND DISCUSSION

Although some limitations of the coupled gas-liquid DNS for this developing turbulent boundary layer typed flow with the free-surface deformation, some preliminary results of turbulent statistics for the free-surface, pressure distribution, velocity fluctuations, two-point correlation, energy spectrum and budget of turbulent kinetic energy are obtained.

Figures 2(a) and 2(b) show the snap-shots of the instantaneous free-surface behavior at 18.15 sec, which is near the end of computation, for an overall-view of the free-surface configuration, a side-view of the free-surface shape and the normalized velocity field and a cross-section view of the secondary flow in the x-y plane, respectively. The flow direction is the left to the right in the figure. As shown in Fig.2(a), many ripples and small waves are generated on the free-surface and some of them are growing up to the big waves. Finally, many small ripples on the long wave, some breaking-up waves, some liquid-droplets in the gas-flow and some bubbles in the liquid-flow are observed. It can be seen in Fig. 2(b) that the strong secondary flows in the gas-flow interact with the liquid-flow through the free-surface. The momentum may transfer from the gas- to the liquid-side through the free-surface and vice versa. The secondary flow is suppressed near the bottom region of the liquid-side because of the hydrostatic pressure (as shown in Fig. 4(a)).

Figures 3(a) and 3(b) show the mean and fluctuation (rms) distributions of the free-surface position. The mean free-surface F_{mean} is existing from around y=1.7 m to 2.6 m and the peak of the free-surface fluctuation F_{rms} is located at around y=2.1 m. The upper-shift of the free-surface position can be considered that the lifting force is caused by the Kelvin-Helmholtz instability because the lower pressure regions appear on the top of the waves.

The mean pressure P_{mean} and pressure fluctuation P_{rms} distributions along the y-direction are shown in Figs. 4(a) and 4(b), respectively. In liquid-side, the mean pressure profile shows the typical hydrostatic pressure distribution. The high pressure fluctuation appears underneath the free-surface and may correspond to the conclusions of previous many investigations despite no-deformation of the free-surface, i.e., the free-surface turbulence structure is dominated by the shear rate consideration in the liquid-side. However, the pressure fluctuation is mainly caused by the fluctuation of the free-surface deformation due to the coupled effect between gas- and liquid-flow.

Figure 5 shows the mean axial velocity (w_{mean}) profile along the y-direction. The velocity near the bottom of computational domain is very small because of the hydrostatic pressure. The velocity profile shows that the gas-flow region is a developing turbulent boundary layer. It means the computational domain in the gas-side is considered to be small, however, the number of the computational grids used in this study is the maximum in our computer system, i.e., the vector-parallel supercomputer Fujitsu VPP500-16 processor elements which can be used around 3 Giga bytes.

The velocity fluctuation (rms) distributions are shown in Fig. 6. It is found that the v_{rms} which is the velocity component normal to the free-surface is larger than the spanwise fluctuation (u_{rms}) in the free-surface region. This large v_{rms} in both gas- and liquid-side could be produced a substantial amount of the turbulent kinetic energy at the free-surface. This is a new turbulent energy production mechanism that has been never observed in the previous studies, i.e., the first numerical observation via DNS with free-surface deformation.

In order to grasp the turbulent feature from energy cascade point of view, the energy spectra $S_{ii}(k_z)$ $S_F(k_z)$ for three velocity components and F-value at the free-surface region are shown in Figs. 7(a) for streamwise; $S_{ii}(k_z)$ and $S_F(k_z)$, and 7(b) for spanwise wave-numbers; $S_{ii}(k_x)$ and $S_F(k_x)$, respectively. All the spectra in Figs. 7(a) and 7(b) are shown in the range of up to k_z=16 because of the spatial resolution, i.e., the maximum wave-numbers k_x=k_z=16. The spanwise spectra in Fig. 7(b) indicate a quasi-two-dimensional turbulence because there is a $k^{-5/3}$ region at relatively high wave number. The streamwise spectra in Fig. 7(a) for the velocity components are strongly dissipated because there is a $k^{-4.5}$ region at relatively high wave number. These results are similar to that of Banerjee (1994). However, the F-spectrum regarding the free-surface deformation indicates the quasi-two-dimensional turbulence because there is a $k^{-5/3}$ region. This means the free-surface behaves the quasi-two-dimensional turbulence despite the velocity components being strongly dissipated .

The turbulent kinetic energy budget is shown in Fig. 8. The total budget is not well-balanced because the number of sampling is not enough in this preliminary study and this flow is a developing boundary layer typed flow. However, the tendency of the energy budget of the turbulent free-surface flow with high shear wind can be discussed qualitatively.

As expecting from the results above mentioned, the large amount of turbulence energy is produced in the free-surface deformation region and the viscous diffusion and dissipation terms are very small except near the upper boundary where v-velocity is set to be zero and the gradient of other quantities are set to be zero, i.e., the free-slip condition is imposed. The pressure-diffusion is highly changed in the free-surface region and is almost balanced with the turbulent diffusion. The major interest in this budget might be the effect of the turbulent convection on the turbulent production. The convection term caused by the mean velocity is not appeared in the ordinary turbulent kinetic energy budget for the wall-turbulence flows. However, the mean velocity in case of the turbulent free-surface flow with high velocity wind is highly changed in both the free-surface region and the upper region of the gas-side as shown in Figs. 5 and 6. Therefore, the correlation between the fluctuating wavy-motion on the free-surface and the large change of the velocity there, i.e., turbulent convection, may lead to produce large amount of turbulent kinetic energy in the free-surface region.

Finally, the vortexes observed here may be generated by high shear stresses at the free-surface region and transferred from the free-surface, however it cannot be shown in this paper because of the limitation of paper length. Similar vortex motions have been observed by Banerjee (1994) and Pan and Barnerjee (1995) despite no consideration of the surface deformation and the hydrostatic pressure gradient, such as the open channel flows. According to Pan and Banerjee (1995), "If turbulence generation at bottom wall is turned off, the upwellings (related to bursts) and downdrafts no longer form." However, the flow pattern and turbulent structure underneath the free-surface observed in this study having no bottom solid wall are something similar to that of Barnerjee (1994) and Pan and Banerjee (1995). It should be necessary to investigate the reason why both turbulent structures are similar despite the different boundary conditions and turbulent production processes. These vortex generation and movement mechanisms would have a very important role for the turbulent scalar transfer, especially the carbon-dioxide gas transport from air to the sea.

CONCULING REMARKS

A DNS on a turbulent free-surface flow with the high shear wind has been carried out to grasp and understand a gas-liquid interaction mechanism by means of the MARS. According to this preliminary DNS results, the free-surface is strongly deformed by the high shear stresses between two flows. Many small ripples on the big waves, some breaking-up waves, some liquid-droplets in the gas-flow and some bubbles in the liquid flow are observed. The statistics of the turbulent quantities for the turbulent free-surface flow are obtained numerically. It is found that the turbulent energy is produced by the fluctuating wavy-motion of the free-surface, i.e., the fluctuation of the free-surface deformation, the normal velocity fluctuation (v_{rms}) and the turbulent convection. This large v_{rms} generated in both gas- and liquid-side is produced a substantial amount of the turbulent kinetic energy in the free-surface region. This new mechanism regarding the turbulent energy production is the first numerical finding via DNS with the free-surface deformation. However, it is necessary to investigate more detailed turbulent structure.

The preliminary results indicate the effects of turbulent free-surface structure on the momentum transport are very strong and could be very important to grasp the scalar transport through the free-surface like a gas-absorption regarding the global climate/environment problems.

REFERENCES

Banerjee, S., 1994, "Upwellings, downdrafts, and whirlpools: Dominant structures in free surface turbulence," *Appl. Mech. Rev.* vol. 47, No.6, Part 2, pp.S166-S172.

Brackbill, J.U., Kothe, D.B., and Zemach, C., 1992, "A Continuum Method for Modeling Surface Tension," *J. Comput. Phys.*, vol. 100, pp. 335-354.

Komori, S., Murakami, Y., and Ueda, H., 1989, "The relationship between Surface-Renewal and Bursting Motions in an Open-Channel Flow, *J. Fluid Mech.*, vol. 203, pp.103, 1989.

Kohte, D. B., Rider, W. J., Mosso, S. J., Brock, J. S., and Hochstein, J. I., 1996, "Volume Tracking of Interfaces having Surface Tension in Two and Three Dimensions," *Technical Report AIAA* 96-0859.

Kunugi, T., 1997, "Direct Numerical Algorithm for Multiphase Flows with Free Surfaces and Interfaces, *Proc. ISAC'97 High Performance Computing on Multiphase Flows*, Y. Matsumoto et al., ed., JSME, pp.25-30.

Landau, L. D., and Lifshitz, E. M., 1993, "Fluid Mechanics," 2nd ed., Course of Theoretical Physics, Pergamon Press, Oxford, vol. 6, chap. VII.

Lombardi, P., Angelis, V. D., and Banerjee, S., 1996, "Direct Numerical Simulation of Near-Interface Turbulence in Coupled Gas-Liquid Flow," *Phys. Fluids*, vol. 8, pp. 1643-1665.

Lam, K., and Banerjee, S., 1992, "On the Condition of Streak Formation in a Bounded Turbulent Flow," *Phys. Fluids*, A, vol. 4, pp. 306.

Pan, Y. and Banerjee, S., 1995, "A Numerical Study of Free-Surface Turbulence in Channel Flow," *Phys. Fluids*, vol.7, pp.1649-1664.

Rashidi, M., and Banerjee, S., 1988, "Turbulence Structure in Free-Surface Channel Flows," *Phys. Fluids*, vol. 31, pp.2491.

Satake, S., 1998, Private Communication.

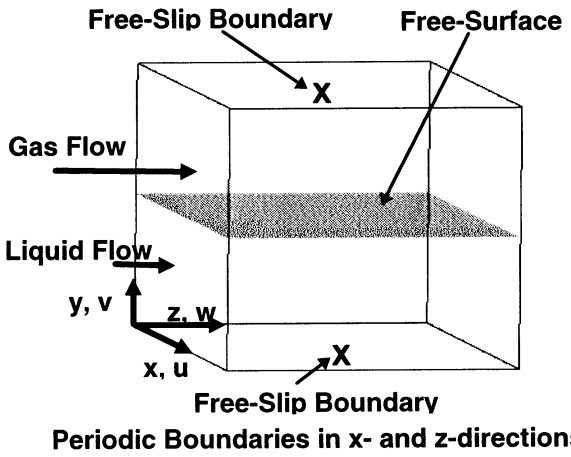

Figure 1. Coordinate System and Boundary Conditions for Turbulent Free-Surface Flow

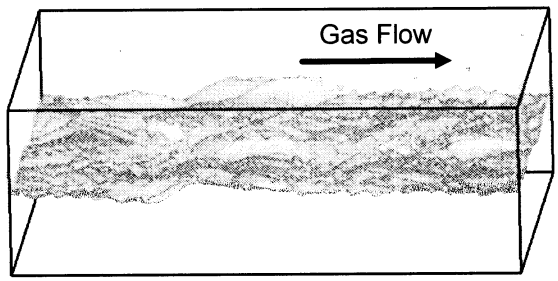

(a) A Snap-shot of the Instantaneous Free-Surface Behavior at t=18.15 sec

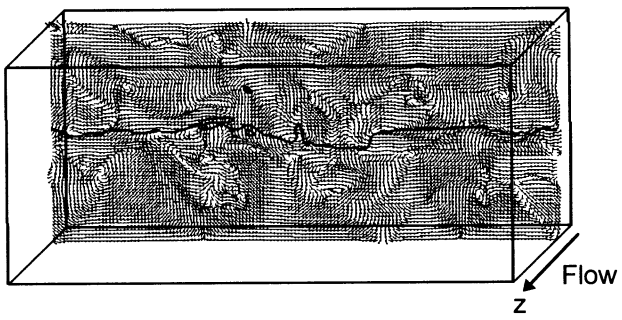

(b) Expanded Cross-section View of the Secondary Flow in the x-y Plane at z=9.125 m

Figure2. Instantaneous Turbulent Free-Surface Motion at t=18.15 sec.

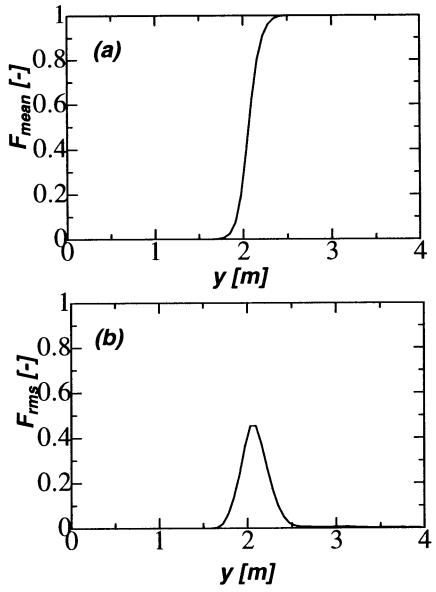

Figure 3. Statistics for Free-Surface Location:(a) Mean Location, F_{mean} and (b) rms Location Fluctuation, F_{rms}

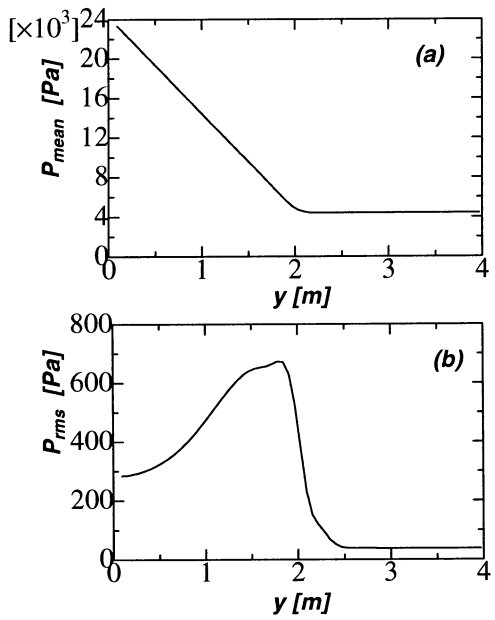

Figure 4. Pressure Distribution; (a) Mean Pressure, P_{mean}, (b) rms Pressure Fluctuation, P_{rms}

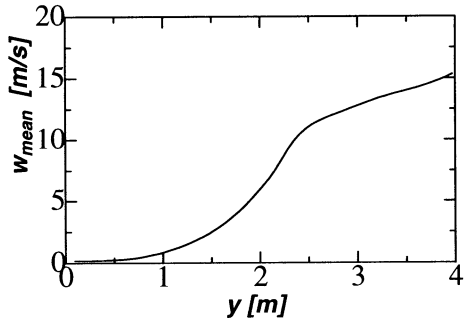

Figure 5. Mean Streamwise Velocity Profile

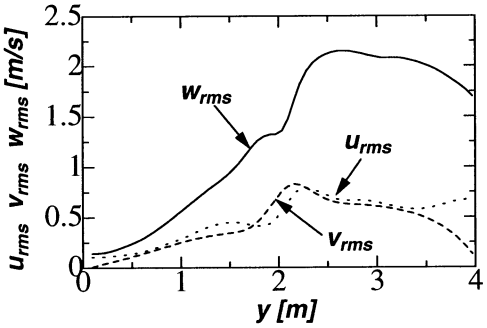

Figure 6. rms Velocity Fluctuations

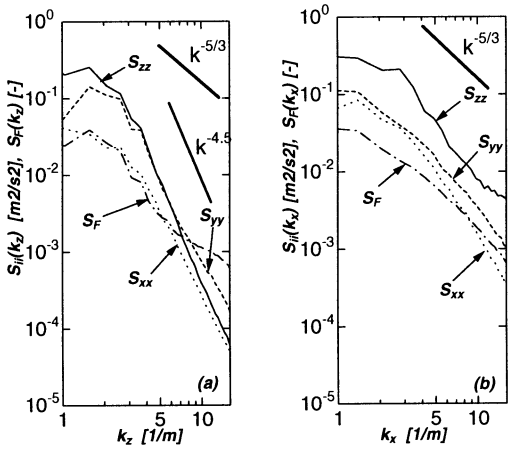

Figure 7. Energy Spectrum for Three Velocity Components and F-value in the Free-Surface Region (at y=2.04 m)

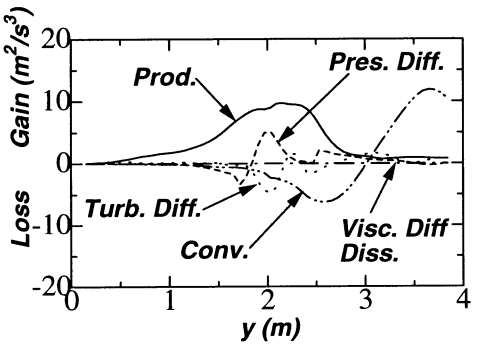

Figure 8. Turbulent Kinetic Energy Budget